

Recent milestones from STAR: new developments and open questions

Rongrong Ma^{1,*} (For the STAR Collaboration)

¹Brookhaven National Laboratory, Upton, NY 11973, USA

Abstract. In these proceedings, an overview of recent STAR results on selected topics is presented. These results utilize Au+Au collisions at various energies, and are aimed at understanding the properties of QED and QCD, characterizing the quark-gluon plasma, as well as searching for the possible critical point in the QCD phase diagram. Specifically, following measurements are discussed: global hyperon polarization, net-proton fluctuations, low transverse momentum dimuon pair production, hyperon-baryon correlations, and $f_0(980)$ elliptic flow.

1 Introduction

The Quark-Gluon Plasma (QGP), consisting of deconfined quarks and gluons, can be created through a phase transition from ordinary nuclear matter in which quarks and gluons are confined within hadrons. This transition is realized at the Relativistic Heavy Ion Collider (RHIC) in head-on collisions of high energy Au beams. At top center-of-mass energy per nucleon-nucleon pair, i.e. $\sqrt{s_{NN}} = 200$ GeV, the main physics goal of the RHIC program is to confirm the QGP formation and study its properties. Additionally, the Beam Energy Scan (BES) program, consisting of two phases, is designed to explore the QCD phase diagram and search for a possible critical point, using Au+Au collisions down to 7.7 GeV (3.0 GeV) in collider (fixed-target) mode. In recent years, heavy-ion collisions and the QGP are also used to carry out research beyond traditional heavy-ion physics, such as coherent photon-photon processes, hyperon-nucleon interactions, etc.

In these proceedings, recent developments from the Solenoidal Tracker at RHIC (STAR) experiment [1] are presented. Physics implications of these results and remaining open questions are discussed along the way.

2 QGP and critical point search

2.1 Global hyperon polarization

In 2017, a new phenomenon of global polarization for both Λ and anti- Λ hyperons, shown as open and filled circles in the left panel of Fig. 1, was discovered in mid-central Au+Au collisions [2]. Such a global polarization is believed to be induced by the vorticity of the medium, which aligns the spins of Λ and anti- Λ along the system's initial orbital momentum direction. A hint of a rising trend of the global polarization with decreasing collision energy is seen, whose confirmation requires measurements of better precision at low energies.

*e-mail: marr@bnl.gov

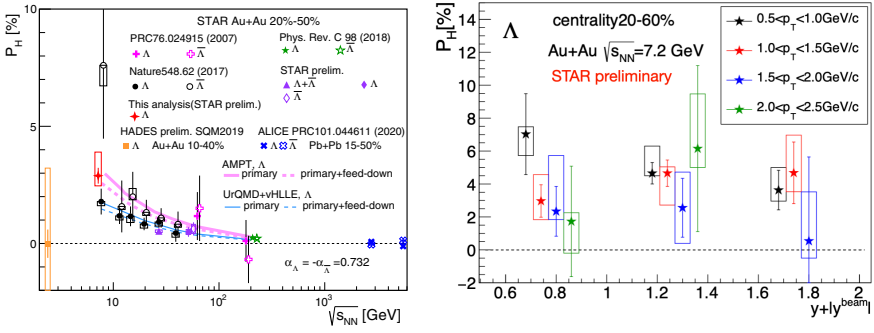


Figure 1. Left: collision energy dependence of global polarization for Λ and anti- Λ in mid-central Au+Au collisions. Right: rapidity dependence of the Λ global polarization in 20-60% central Au+Au collisions at $\sqrt{s_{NN}} = 7.2$ GeV.

The latest measurement of the Λ global polarization in 7.2 GeV Au+Au collisions is shown as the red star in Fig. 1, left panel. Its value is consistent with previous measurement at 7.7 GeV but with better statistical precision, and also consistent with increasing polarization at lower energies. To better understand how the system’s angular momentum couples with the hyperon spin, studying the rapidity dependence of the global polarization is of great interest. Dominance of the initial local orbital angular momentum driven by the collision geometry would lead to an increase of the global polarization with rapidity [3], while local thermal vorticity and hydrodynamic evolution predict a decreasing trend or weak dependence with rapidity [4]. The right panel of Fig. 1 shows the Λ global polarization as a function of rapidity in 20-60% central Au+Au collisions at $\sqrt{s_{NN}} = 7.2$ GeV. Within the large experimental uncertainties, no obvious rapidity dependence is seen. The data set taken during BES-II with more statistics and a larger rapidity coverage will significantly improve the precision of rapidity dependence measurement.

Since the Λ global polarization arises from the coupling between the system’s angular momentum and particle spin, other hyperons should show similar behavior. Figure 2 shows the measurements of global polarizations for Ξ and Ω in 20-80% central Au+Au collisions at $\sqrt{s_{NN}} = 200$ GeV [5]. Results for particles and anti-particles are combined. The Ξ polarization

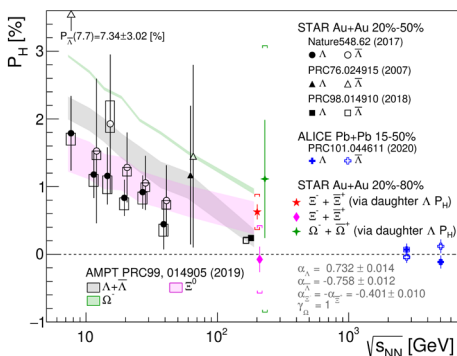


Figure 2. Measurements of global polarizations for Ξ and Ω in 20-80% central Au+Au collisions at $\sqrt{s_{NN}} = 200$ GeV [5]. They are compared with similar measurements for Λ at both RHIC and the LHC.

is measured in two ways, via analysis of the angular distribution of the daughter particles (magenta diamond) and via measuring the polarization of the daughter Λ -hyperon (red star). The average of the two gives Ξ global polarization of $\langle P_{\Xi} \rangle = 0.47 \pm 0.10(\text{stat.}) \pm 0.23(\text{syst.})\%$.

The Ω global polarization is measured to be $\langle P_\Omega \rangle = 1.11 \pm 0.87(\text{stat.}) \pm 1.97(\text{syst.})\%$. Despite the large uncertainties, the positive values are consistent with the underlying mechanism that the system's vorticity induces the observed global polarization.

2.2 Search for the critical point

Searching for the possible critical endpoint in the QCD phase diagram is one of the main goals of the BES program at RHIC. One promising tool is to study fluctuations of conserved quantities, such as the baryon number, whose correlation lengths diverge at the critical point. Experimentally, ratios of high-order moments of net-proton multiplicity distribution, i.e. number of protons minus that of anti-protons, are used, and results are shown in Fig. 3 [6]. The left and right panels show the skewness times variance ($S\sigma = C_3/C_2$) and kurtosis times variance square ($\kappa\sigma^2 = C_4/C_2$) as a function of collision energy, respectively using BES-I data, where C_n is the n^{th} moment of the net-proton distribution. Results from 0-5% (filled circles) and

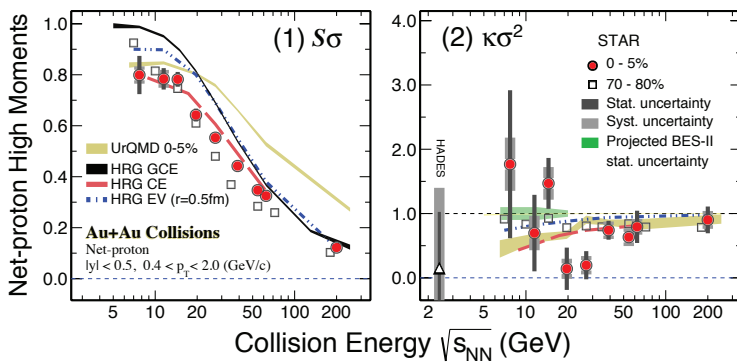


Figure 3. Collision energy dependence of net-proton $S\sigma$ (left) and $\kappa\sigma^2$ (right) in 0-5% (filled circles) and 70-80% (open squares) Au+Au collisions [6].

70-80% (open squares) Au+Au collisions are shown, where the latter is used as a reference for the case of no critical point. A non-monotonic behavior is seen for $\kappa\sigma^2$ in 0-5% central collisions with a significance of 3.1σ , consistent with the expectation of the presence of the critical point, while the 70-80% result shows little dependence on collision energy.

Collision energy dependence of even higher-order moment ratio (C_6/C_2), presumably more sensitive to the correlation length, is shown in Fig. 4. Theoretical calculations predict negative C_6/C_2 values when a phase transition between hadronic and partonic matter occurs [7]. The measured values are positive for 70-80% peripheral collisions, while they are negative for 0-40% central collisions at most energies. Enhanced statistics from BES-II is of great importance to these measurements.

3 Explore new physics with heavy-ion collisions

3.1 Photon-photon process

In ultra-relativistic Au+Au collisions, large fluxes of linearly polarized photons are emitted by incoming highly-charged nuclei. Consequently, coherent photon-photon interactions would occur, producing excess dilepton pairs above known hadronic sources at very low transverse momentum (p_T). Such a process has been observed in the dielectron channel

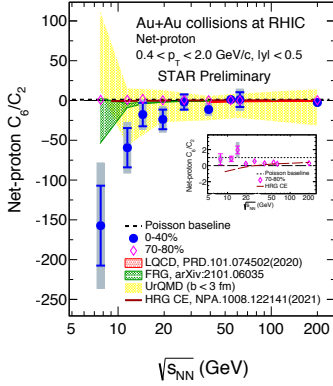


Figure 4. Collision energy dependence of net-proton C_6/C_2 in 0-40% (filled circles) and 70-80% (open diamonds) Au+Au collisions.

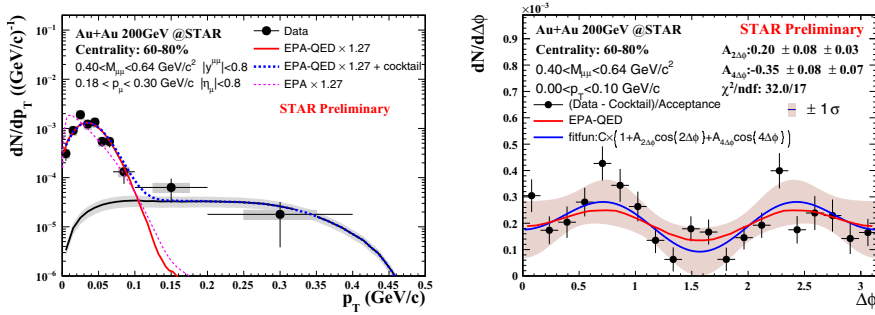


Figure 5. p_T (left) and azimuthal (right) distributions of dimuon pairs in 60-80% peripheral Au+Au collisions at $\sqrt{s_{NN}} = 200$ GeV. See text for the definition of the azimuthal angle.

[8, 9], and new complimentary measurements via the dimuon channel are shown in Fig. 5. The left panel shows the p_T distribution of dimuon pairs with the pair mass between 0.40 and 0.64 MeV/c^2 in 60-80% peripheral Au+Au collisions at $\sqrt{s_{NN}} = 200$ GeV. Compared to the known hadronic sources (black solid curve), a clear excess at $p_T < 0.1$ GeV/c is seen, which is a signature of coherent photon-photon interactions. Theoretical calculations based on QED are consistent with the data within uncertainties [10].

Since colliding photons are linearly polarized, $\cos(2\Delta\phi)$ and $\cos(4\Delta\phi)$ modulations are expected for the produced dilepton pairs [11], where $\Delta\phi$ is the angle between the momenta of the lepton pair and the positively charged lepton. The $\cos(4\Delta\phi)$ modulation has been observed in the dielectron channel [9], while the $\cos(2\Delta\phi)$ modulation is easier to be measured in the dimuon channel since it is suppressed by the power of m^2/p_T^2 for the electron channel. The $\Delta\phi$ distribution for low- p_T dimuon pairs is shown in the right panel of Fig. 5. A fit to the distribution yields a compatible $\cos(4\Delta\phi)$ modulation to the dielectron result, and a first observation of $\cos(2\Delta\phi)$ modulation with a significance of 2.3σ .

3.2 Hyperon-baryon interactions

Understanding interactions between hyperons and baryons will provide important inputs to resolving the “hyperon puzzle” in neutron star research. Such measurements can be carried out in heavy-ion collisions as hyperons and baryons are copiously produced in these collisions. The left panel of Fig. 6 shows the ratio of the p - Ξ correlations in peripheral and

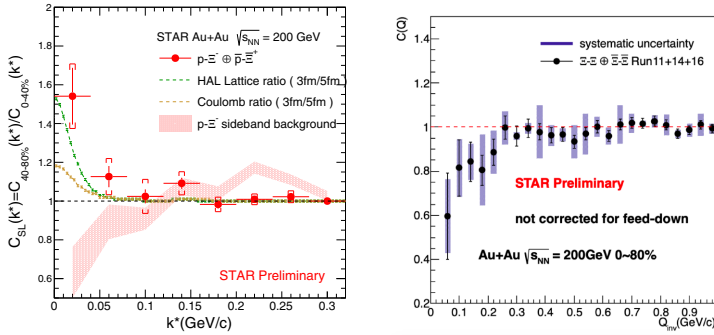


Figure 6. Left: ratio of p - Ξ correlation between peripheral and central Au+Au collisions at $\sqrt{s_{NN}} = 200$ GeV as a function of half of relative momentum between p - Ξ pair in the pair rest frame. Right: correlation of Ξ - Ξ as a function of relative momentum in 0-80% Au+Au collisions at $\sqrt{s_{NN}} = 200$ GeV.

central Au+Au collisions at $\sqrt{s_{NN}} = 200$ GeV as a function of k^* , which is half of the relative momentum between the p - Ξ pair in the pair rest frame. Compared to the baseline calculation taking into account the Coulomb interaction (orange dashed line) [12], the data indicate additional attractive strong interaction between p and Ξ for $k^* < 0.05$ GeV/c, which is consistent with lattice QCD calculation (green dashed line) [13]. Furthermore, the correlation between $\Xi - \Xi$ pairs is studied in 0-80% 200 GeV Au+Au collisions, and the result is shown in the right panel of Fig. 6. A hint of negative correlation at small relative momentum is seen. Additional studies on feed-down contribution and Coulomb effect are needed to better interpret the data.

3.3 $f_0(980)$ quark content

Despite being observed in 1970's, the exact quark content of $f_0(980)$ meson remains an open question. Different scenarios include standard $q\bar{q}$, tetraquark, meson-meson bound state, or gluon ball, or a superposition of these states. In Au+Au collisions at RHIC, particle's elliptic flow (v_2) is seen to empirically follow the number of constituent quark (NCQ, n_q) scaling, i.e. v_2/n_q collapses to a common curve for different particles when plotted against $(m_T - m_0)/n_q$, where $m_T = \sqrt{m_0^2 + p_T^2}$ and m_0 is the particle's rest mass. This is because v_2 is mainly developed during the partonic phase before hadronization. In turn, one can use this scaling property to infer the quark content of $f_0(980)$ by examining its v_2 . Results are shown in Fig. 7, in which both two- and four-quark assumptions are used. Using the common trend by fitting the results for other particles, the inferred number of constituent quarks is $3.0 \pm 0.7(\text{stat.}) \pm 0.5(\text{syst.})$, which is inconclusive due to large uncertainties. Additional data taking of 200 GeV Au+Au collisions planned for 2023 and 2025 will be beneficial in reducing uncertainties of this measurement.

4 Summary

These proceedings present recent developments from the STAR experiment at RHIC. Significant global polarization for Λ is measured in 7.2 GeV Au+Au collisions without any strong rapidity dependence. For Ξ and Ω , positive global polarizations are also seen in 200 GeV

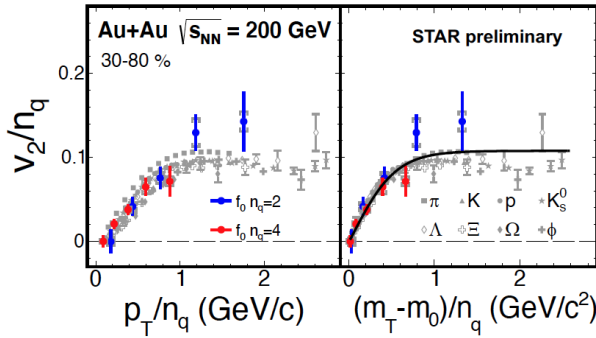


Figure 7. $f_0(980) v_2/n_q$ as a function of quark number scaled p_T (left) and transverse kinetic energy (right). Measurements for other hadrons are shown for comparison.

Au+Au collisions. From the BES program, net-proton kurtosis exhibits a non-monotonic behavior against collision energy, consistent with the expectation of a QCD critical point. Furthermore, low- p_T dimuon pair production, arising from coherent photon-photon interactions, is observed, and reveals a $\cos(2\Delta\varphi)$ modulation due to the linear polarization of the incoming photons. An indication of attractive strong interaction between p and Ξ at low relative momenta is seen, which provides important inputs to neutron star studies. Last but not least, the $f_0(980) v_2$ is checked for NCQ scaling, but a firm conclusion requires better precision. Datasets taken during BES-II and future data-taking at top energy will greatly improve the precision of these measurements.

References

- [1] K.H. Ackermann et al. (STAR), Nucl. Instrum. Meth. A **499**, 624 (2003)
- [2] L. Adamczyk et al. (STAR), Nature **548**, 62 (2017), 1701.06657
- [3] Z.T. Liang, J. Song, I. Upsal, Q. Wang, Z.B. Xu, Chin. Phys. C **45**, 014102 (2021), 1912.10223
- [4] W.T. Deng, X.G. Huang, Phys. Rev. C **93**, 064907 (2016), 1603.06117
- [5] J. Adam et al. (STAR), Phys. Rev. Lett. **126**, 162301 (2021), 2012.13601
- [6] J. Adam et al. (STAR), Phys. Rev. Lett. **126**, 092301 (2021), 2001.02852
- [7] W.j. Fu, X. Luo, J.M. Pawlowski, F. Rennecke, R. Wen, S. Yin (2021), 2101.06035
- [8] J. Adam et al. (STAR), Phys. Rev. Lett. **121**, 132301 (2018), 1806.02295
- [9] J. Adam et al. (STAR) (2019), 1910.12400
- [10] W. Zha, J.D. Brandenburg, Z. Tang, Z. Xu, Phys. Lett. B **800**, 135089 (2020), 1812.02820
- [11] C. Li, J. Zhou, Y.J. Zhou, Phys. Lett. B **795**, 576 (2019), 1903.10084
- [12] K. Morita, A. Ohnishi, F. Etminan, T. Hatsuda, Phys. Rev. C **94**, 031901 (2016), [Erratum: Phys.Rev.C 100, 069902 (2019)], 1605.06765
- [13] T. Hatsuda, K. Morita, A. Ohnishi, K. Sasaki, Nucl. Phys. A **967**, 856 (2017), 1704.05225